Ilicicolinic acids and ilicicolinal derivatives from the fungus Neonectria discophora SNB-CN63 isolated from the nest of the termite Nasutitermes corniger found in French Guiana show antimicrobial activity

Jonathan Sorres, Abir Sabri, Orianne Brel, Didier Stien, Véronique Eparvier

Ilicicolinic acids and ilicicolinal derivatives from the fungus *Neonectria discophora* SNB-CN63 isolated from the nest of the termite *Nasutitermes corniger* found in French Guiana show antimicrobial activity

Jonathan Sorres[a], Abir Sabri[a], Orianne Brel[a], Didier Stien[b], Véronique Eparvier[a,]*

[a] *CNRS, Institut de Chimie des Substances Naturelles, UPR 2301, Université Paris-Saclay, 1 avenue de la Terrasse, 91198 Gif-sur-Yvette, France*

[b] *Sorbonne Universités, UPMC Univ. Paris 06, CNRS, Laboratoire de Biodiversité et Biotechnologies Microbiennes (LBBM), Observatoire Océanologique, 66650 Banyuls/Mer, France*

[*] *Corresponding author: Tel: +33 1 69 82 36 79. Fax: +33 1 69 82 37 84. E-mail address: veronique.eparvier@cnrs.fr (V. Eparvier)*

1. Introduction

The search for antimicrobial molecules represents a global challenge in public health. Then, the emergence of multiresistant pathogenic microbial strains and the global increase of the incidence of bacterial and fungal infections encourage the search for new antibiotic compounds (Martinez-Rossi et al., 2008; Davies et al., 2013). Novel lead-like antibiotic molecules, in particular those drugs belonging to new structural classes, are urgently needed (Borysowski and Górski 2008). Recently, the exploration of the chemical basis and well-described bacteria-host or fungal-host interactions have been shown to be a powerful strategy to identify novel chemical entities, in particular, in natural products from microbes like fungi associated with insects (Beemelmanns et al., 2016; Rhamadar et al., 2014; Nirma et al., 2013; Adnani et al., 2017). In fact, insects are the most diverse animal groups on earth (Purvis and Hector, 2000). Social insects, particularly ants, are well studied for their symbiosis with microbes to protect colonies (Berenbaum and Eisner, 2008; Stow et al., 2007, 2008; Currie et al., 2006). These mechanisms are also described with termites (Matsui et al., 2012; Nirma et al., 2013, Nirma et al., 2015). Therefore, the symbiotic nature of some fungi favours metabolic interactions with their host and environment, thereby increasing the production of bioactive compounds (Beemelmanns et al., 2016; Adnani et al., 2017).

In a preceding study, we isolated *Neonectria discophora* fungus from a termite nest. This strain was chemically studied, and we isolated the new antibacterial ilicicolinic acids (C and D) and the original structure named ilicicolonal (Nirma et al., 2015a). These molecules, with 5-chloro-2,4-dihydroxy-6-methylbenzoic acid or 5-chloro-2,4-dihydroxy-6-methylbenzaldehyde moieties, such as aschochlorins, ascofurons, colletochlorins, ilicicolinic acids and ilicicolins, are less represented in the literature and are isolated from diverse macroscopic and microscopic fungi genuses in association with plants, sponges or insects (Beemelmanns et al., 2016; Takamatsu et al., 1994; Gutiérrez et al., 2005; Zhang et al., 2009). These compounds show inter alia cytotoxicity on cancer cells lines and antimicrobial activities (Hashimoto et al., 2005; Beemelmanns et al., 2016).

2. Results and Discussion

During our first work on *Neonectria discophora*, many potentially new compounds were detected in the active fractions by LC-MS (Nirma et al., 2015a). The amount of extract available was, however, too low to isolate these molecules, establish their structures and evaluate their biological activities. We then decided to reinvestigate this strain chemically. The bioguided fractionation allowed us to isolate the known ilicicolinal (**1**) and ilicicolin A, also named LL-Z1272α (**2**), which were identified by comparison with literature data, (Mori and Fujioka, 1984; Ellestad et al., 1969; Kawagachi et al., 2013) along with 12 new derivatives of ilicicolin and ilicicolinic acids **3**-**14** (Fig. 1).

Compound **3** was obtained as a dark purple oil. Its molecular formula ($C_{23}H_{31}ClO_4$) was determined by HRESIMS ($[M+H]^+$ peak at *m/z* 407.1991 calcd at *m/z* 407.1989), suggesting eight degrees of unsaturation. The ^1H and ^{13}C NMR spectra revealed similarities to **1** (Table 1 and 2), with only some minor differences observed on the benzoyl group. Therefore, the ^1H-^{13}C HMBC and ^1H-^1H COSY correlations of **3** were similar to **1** (Fig. 2). However, we observed for compound **3** a hydroxyl proton at δ_H 8.59 contrary to a hydroxyl at 12.50 ppm for **1**. This fact, permitted to determinate that compound **3** is cyclized on benzoyl group on C-2 contrary to compound **3,** which was cyclized on C-4. This compound was named ilicicolinal B.

Compound **4** was obtained as a yellow oil. Its molecular formula ($C_{23}H_{31}ClO_4$) was determined by HRESIMS ($[M-H]^-$ peak at *m/z* 405.1821, calcd 405.1833), suggesting eight degrees of unsaturation. The ^1H and ^{13}C NMR spectrums were similar to that of compound **2** (Table 1 and 2). The main difference was its localization on the side chain since there was only one methylene carbon at C-9′ at δ_C 27.0 ppm. COSY correlations between H-9′ and the protons H-8′ and H-10′, in addition to the HMBC correlations between H-9′ and the carbons C-7′, C-8′ and C-10′, led to a di-unsaturated hydrocarbon chain on C-8’ and C-10’ (Fig. 2). To access the cyclopentane structure, we first noticed the COSY correlations between H-6′ at δ_H 2.49 ppm and the protons H-2′ and H-5′ at δ_H 1.90 and 1.83 ppm, respectively. The methylene 3′-CH_3 at δ_H 1.03 ppm had HMBC correlations with the carbons C-2′, C-3′ and C-4′, which allowed the cyclization into C-6’. This was well supported by the H-5′ HMBC correlations with the carbons C-2′ and C-6′. The presence of the carbinol at position C-3’ was suggested by the deshielded chemical shift at δ_C 80.6 ppm. The nOe correlation observed between the CH_3-3′ and the H-2′, as well as the coupling constant between H-6′ and H-2′ as well as H-5′ at J = 11.0 and 10.3 Hz, respectively, confirm the pseudo-axial position of H-6′ (Fig. 3), and allow us to deduce the relative configuration of the compound **4**.

Compound **5** and **6** were obtained as a dark purple powder. Their molecular formula ($C_{23}H_{31}ClO_4$) was identical to molecule **4** ($[M-H]^-$ peak at *m/z* 405.1828 for **5** and 405.1842 for **6**, respectively, calcd 405.1833). The ^1H and ^{13}C NMR spectra of **5** and **6** were very similar to those of **4** (Table 1 and 2), with only one difference on the carbon side chain. For compound **5**, the ^1H NMR spectra revealed the presence of an exomethylene group at δ_H 4.93 ppm. The HMBC correlations between the proton at 2.15 and 2.83 ppm with the carbon at 150.9 and 110.6 ppm and, ^1H-^1H coupling between δ_H at 2.83 ppm with a proton at 2.12, 2.23 and 5.17 ppm unambiguously positioned this exomethylene in position C-7′ (Fig. 2). In molecule **6**, the difference was localized on the double bond in C-7′. In fact, the clear and intense nOe correlation between the proton of methyl 7’-CH_3 at 1.77 ppm and the olefinic proton H-8’ at 5.30 ppm allowed us to deduce the *Z* configuration for

the C-7'−C-8' double bond. The relative configuration was based on the nOe correlations analysis and by comparison with molecule **4** (Fig. 3). These compounds **4**, **5** and **6** were named ilicicolinal C, D and E.

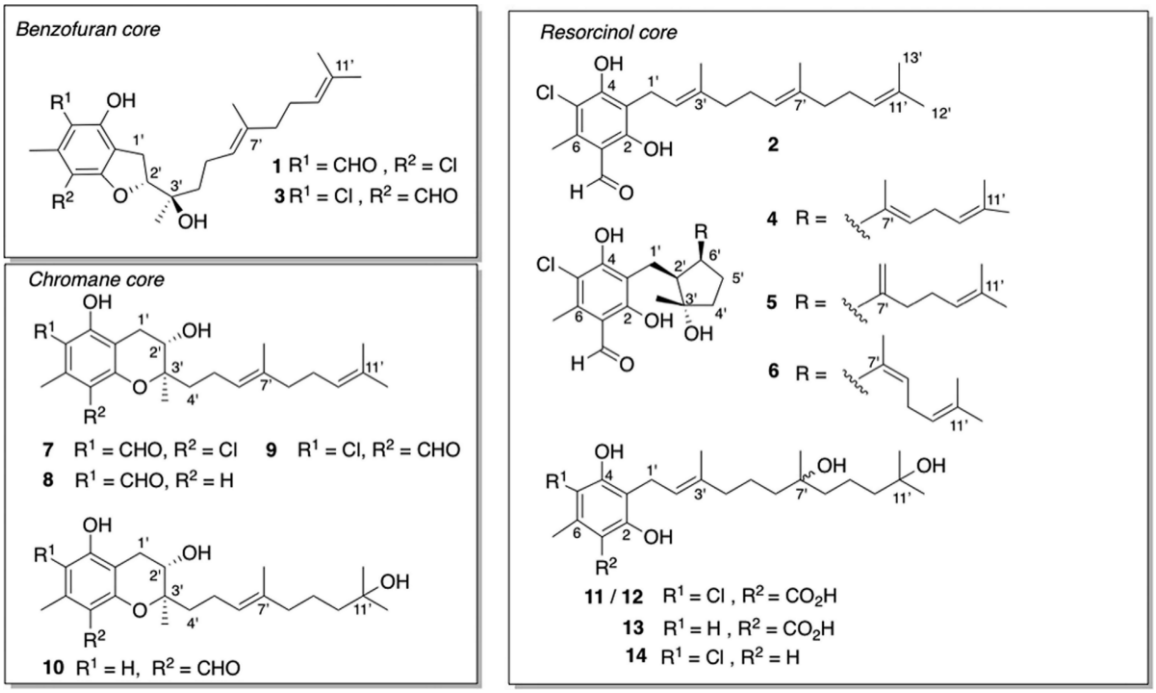

Fig. 1. Structures of isolated compounds **1** to **14**.

Compound **7** was obtained as a brown oil, and its molecular formula was determined to be $C_{23}H_{31}ClO_4$ based on the HRESIMS ($[M+H]^+$ peak at *m/z* 407.1993, calcd 407.1989) corresponding to eight degrees of unsaturation. We first noticed that compound **7** and **2** presented similar ^1H and ^{13}C NMR spectra (Table 2 and 3). The geranyl side chain was easily deduced from the COSY correlations H-4′/H-5′, H-5′/H-6′ and H-9′/H-10′, together with the intense HMBC correlations observed for the protons of methyl 7'-CH_3 with C-6′/C-7′/C-8′ and the protons of methyl 12′-CH_3/13′-CH_3 with C-10′/C-11′ (Fig. 2). The chromane moiety was determined with the COSY correlation H-1′/H-2′ and with the HMBC correlations given by the protons H-1′ with the aromatic carbons C-2/C-3/C-4, the aldehydic proton at 10.14 ppm with C-4/C-5 and the methyl 6-CH_3 with C-1/C-5/C-6. The connection of the geranyl chain was deduced from the HMBC correlations H-4′/H-5′ with the oxygenated quaternary carbon C-3′ and 3′-CH_3 with C-2′/C-3′/C-4′.

Compound **8** was obtained as a yellow oil. Its molecular formula ($C_{23}H_{32}O_4$) was determined by HRESIMS ($[M+H]^+$ peak at *m/z* 373.2374 calcd at *m/z* 373.2379) suggesting eight degrees of unsaturation. Compared to **7**, the molecular formula of **8** indicated the presence of additional hydrogen and the lack of the chlorine. It was confirmed by comparison of the ^1H NMR spectra

between **7** and **8**, which showed a unique difference: a supplementary aromatic proton at δ_H 6.23 ppm (Table 2 and 3) for **8**.

Compound **9** was obtained as a dark purple powder and has the same molecular formula as **7** ($[M+H]^+$ peak at *m/z* 407.1994, calcd 407.1989). The ^1H and ^{13}C NMR spectra revealed similarities to **7** (Table 2 and 3), with only some minor differences observed on the benzoyl group. However, the presence of the hydroxyl proton at δ_H 8.59, contrary to 12.73 ppm in molecule **7,** permitted the determination that compound **9** was cyclized on C-2 (as compound **3**) but not on C-4 as molecules **7** and **1**.

Table 1
^1H NMR Spectroscopic Data for Compounds **1**–**6** (δ_H, *J* in Hz are given in parentheses).

Position	2[a]	3[b]	4[a]	5[b]	6[b]
1′	3.41 d (3.4)	3.19 m	2.84 dd (14.3, 3.6) 2.43 dd (14.3, 11.4)	2.68 dd (14.1, 1.7) 2.39 dd (13.8, 11.7)	2.86 d (12.5) 2.39 d (12.7)
2′	6.42 s	4.98 m	1.90 td (11.0, 3.6)	2.82 td (10.6, 3.8)	2.35 td (12.9, 2.8)
4′	2.01 m	1.56 t (8.9)	1.84 m	1.83 m 1.71 m	1.79 m 1.67 m
5′	2.10 m	2.17 m	1.83 m	1.97 m 1.69 m	2.00 m 1.62 m
6′	5.27 t (6.5)	5.17 t (6.8)	2.49 ddd (11.0, 10.3, 7.4)	2.81 m	3.36 ddd (10.5, 10.5, 7.4)
8′	2.01 m	2.00 t (7.4)	5.27 t (7.0)	2.23 m 2.13 m	5.30 brt (7.0)
9′	2.01 m	2.08 m	2.73 t (6.6)	1.97 m 1.69 m	2.82 t (7.2)
10′	5.08 t (6.5)	5.08 t (7.6)	5.12 t (7.0)	5.16 t (6.0)	5.20 brt (7.0)
12′	1.68 s	1.65 s	1.65 s	1.63 s	1.68 s
13′	1.59 s	1.60 s	1.70 s	1.70 s	1.73 s
1-CHO	10.14 s	10.15 s	10.14 s	10.13 s	10.14 s
2-OH	12.69 s		12.77 s	12.84 s	12.80 s
4-OH	nd	8.59 brs	nd	nd	nd
6-CH_3	2.60 s	2.60 s	2.62 s	2.61 s	2.61, s
3′−CH_3	1.80 s	1.26 s	1.03 s	1.14 s	1.07, s
7′−CH_3	1.58 s	1.61 s	1.64 s		1.77, s
7′−CH_2				4.93 s 5.01 s	

[a] Recorded at 500 MHz in $CDCl_3$.
[b] Recorded at 600 MHz in MeOD.

Table 2
^{13}C NMR spectroscopic data for compounds **2**–**14**.

Position	2[a]	3[c]	4[a]	5[c]	6[c]	7[b]	8[b]	9[c]	10[d]	11[c]	12 [d]	13 [d]	14 [d]
1	113.6, C	114.6, C	113.2, C	113.5, C	113.5, C	112.9, C	113.3, C	116.6, C	115.6, C	106.6,	111.3, C	107.4, C	109.8, CH
2	162.2, C	nd	157.9, C	161.7, C	158.0, C	162.0, C	161.0, C	158.9, C	159.2, C	155.0, C	153.0, C	157.0, C	151.7, C
3	114.4, C	113.8, C	114.2, C	114.0, C	114.7, C	106.3, C	105.0, C	108.4, C	106.3, C	114.0, C	114.1, C	112.0, C	115.1, C
4	156.4, C	160.7, C	162.4, C	163.6, C	162.4, C	155.9, C	164.8, C	160.4, C	162.6, C	162.9, C	163.6, C	165.5, C	154.8, C
5	113.2, C	109.4, C	114.4, C	116.6, C	115.0, C	114.9, C	136.5, CH	108.4, C	110.8, C	113.8, C	114.4, C	111.8, CH	117.7, C
6	137.6, C	143.2, C	138.2, C	139.8, C	138.2, C	138.3, C	141.8, C	139.0, C	140.9, CH	136.0, C	137.7, C	139.8, C	133.4, C
1′	22.0, CH_2	28.2, CH_2	20.5, CH_2	20.5, CH_2	20.0, CH_2	25.3, CH_2	25.0, CH_2	27.5, CH_2	21.6, CH_2	22.5, CH_2	22.9, CH_2	23.0, CH_2	23.3, CH_2
2′	120.7, CH	92.6, CH	49.1, CH	49.1, CH	48.4, CH	67.3, CH	67.3, CH	67.6, CH	66.7, CH	122.2, CH	124.0, CH	125.0, CH	123.2, CH
3′	136.9, C	72.8, C	80.6, C	81.4, C	81.2, C	81.6, C	80.6, C	80.8, C	79.9, C	134.3, C	134.4, C	133.3, C	134.7, C
4′	39.7, CH_2	38.5, CH_2	42.4, CH_2	42.1, CH_2	43.2, CH_2	37.3, CH_2	42.4, CH_2	38.3, CH_2	38.2, CH_2	40.5, CH_2	41.2, CH_2	41.2, CH_2	40.3, CH_2
5′	26.7, CH_2	23.1, CH_2	27.8, CH_2	27.4, CH_2	26.9, CH_2	21.6, CH_2	27.8, CH_2	22.6, CH_2	21.8, CH_2	22.0, CH_2	24.0, CH_2	23.0, CH_2	22.2, CH_2
6′	124.4, CH	125.5, CH	55.3, CH	49.2, CH	43.9, CH	123.4, CH	123.5, CH	125.1, CH	124.4, CH	41.5, CH	40.6, CH	43.1, CH	42.5, CH
7′	135.1, C	136.7, C	135.3, C	149.1, C	135.3, C	136.0, C	135.9, C	135.5, C	135.5, C	72.0, C	72.0, C	70.9, C	71.3, C
8′	39.6, CH_2	41.0, CH	125.2, CH	36.9, CH_2	125.2, CH	39.6, CH_2	39.6, CH_2	41.7, CH_2	40.3, CH_2	41.5, CH_2	42.4, CH_2	43.1, CH_2	42.5, CH_2
9′	26.4, CH_2	27.9, CH_2	27.0, CH_2	27.6, CH_2	26.9, CH_2	26.6, CH_2	27.0, CH_2	27.5, CH_2	22.8, CH_2	18.9, CH_2	18.5, CH_2	19.2, CH_2	18.9, CH_2
10′	124.0, CH	125.5, CH	123.3, CH	124.3, CH	124.1, CH	124.2, CH	123.3, CH	125.1, CH	43.8, CH_2	44.0, CH_2	45.3, CH_2	45.4, CH_2	44.9, CH_2
11′	131.2, C	132.5, C	131.5, C	131.9, C	131.7, C	131.5, C	131.5, C	131.8, C	69.2, C	70.1, C	69.8, C	69.4, C	69.2, C
12′	25.7, CH_3	26.0, CH_3	25.7, CH_3	25.8, CH_3	25.7, CH_3	25.7, CH_3	25.7, CH_3	25.9, CH_3	29.2, CH_3	29.1, CH_3	29.9, CH_3	29.6, CH_3	29.3, CH_3
13′	17.6, CH_3	18.0, CH_3	17.7, CH_3	17.8, CH_3	17.7, CH_3	17.7, CH_3	17.7, CH_3	16.6, CH_3	29.2, CH_3	29.1, CH_3	29.9, CH_3	29.6, CH_3	29.3, CH_3
1-CHO	193.2, C	193.4, C	193.4, C	193.1, C	193.4, C	193.3, C	193.4, C	193.2, C	189.4, C				
1-CO_2H										nd	nd	nd	
6-CH_3	14.4, CH_3	14.4, CH_3	14.4, CH_3	14.2, CH_3	14.3, CH_3	14.3, CH_3	14.4, CH_3	17.5, CH_3	21.5, CH_3	18.8, CH_3	18.4, CH_3	23.8, CH_3	19.8, CH_3
3′−CH_3	16.2, CH_3	22.0 CH_3	28.7, CH_3	29.5, CH_3	28.7, CH_3	18.8, CH_3	28.7, CH_3	18.3, CH_3	17.5, CH_3	15.5, CH_3	15.8, CH_3	15.3, CH_3	15.4, CH_3
7′−CH_3	16.0, CH_3	11.8, CH_3	11.8, CH_3		22.6, CH_3	15.9, CH_3	11.8, CH_3	16.6, CH_3	15.4, CH_3	25.4, CH_3	27.4, CH_3	27.8, CH_3	29.3, CH_3
7′−CH_2				110.4, CH_2									

nd = not determined.
[a] Recorded at 125 MHz in $CDCl_3$.
[b] Recorded at 150 MHz in $CDCl_3$.
[c] Recorded at 150 MHz in MeOD.
[d] Recorded at 150 MHz in C_5D_5N.

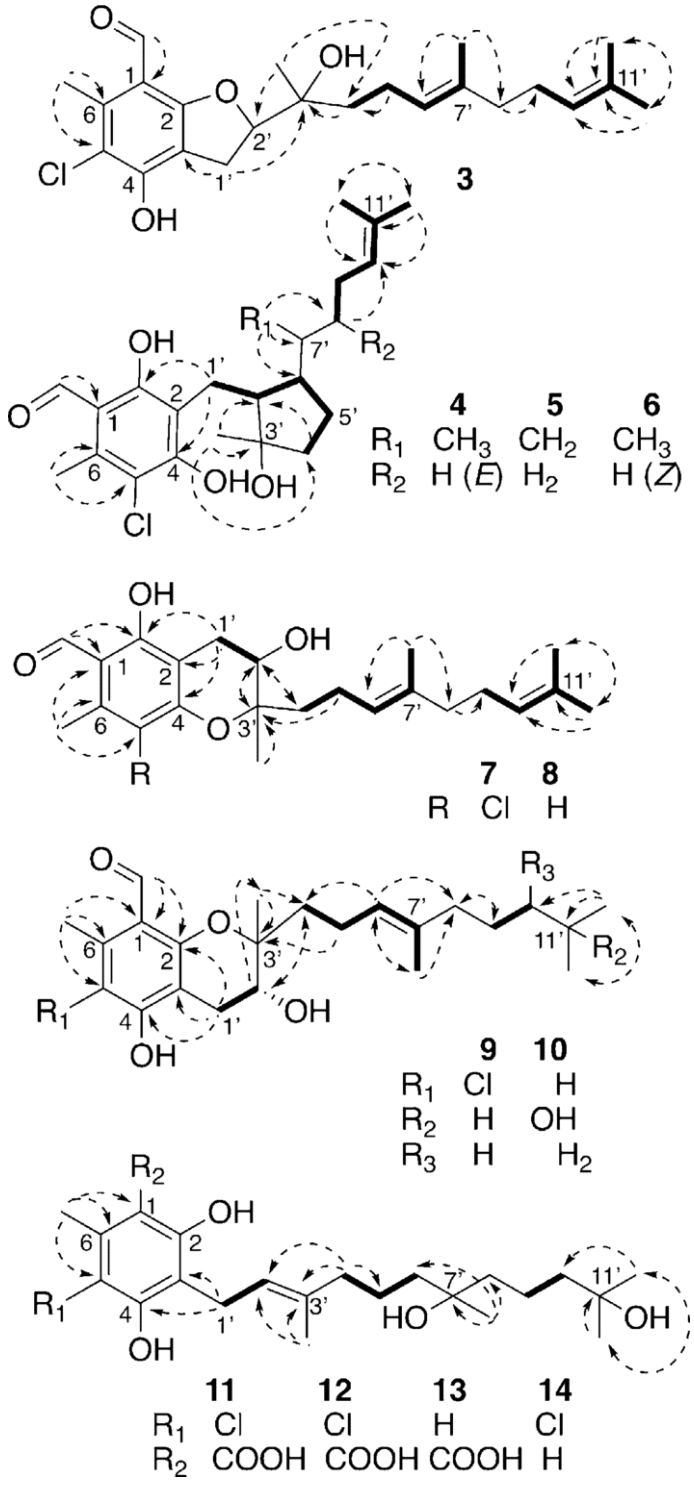

Fig. 2. Key ^{1}H-^{1}H COSY (bold line) and ^{1}H-^{13}C HMBC (dashed arrows) of compounds **3** to **14**.

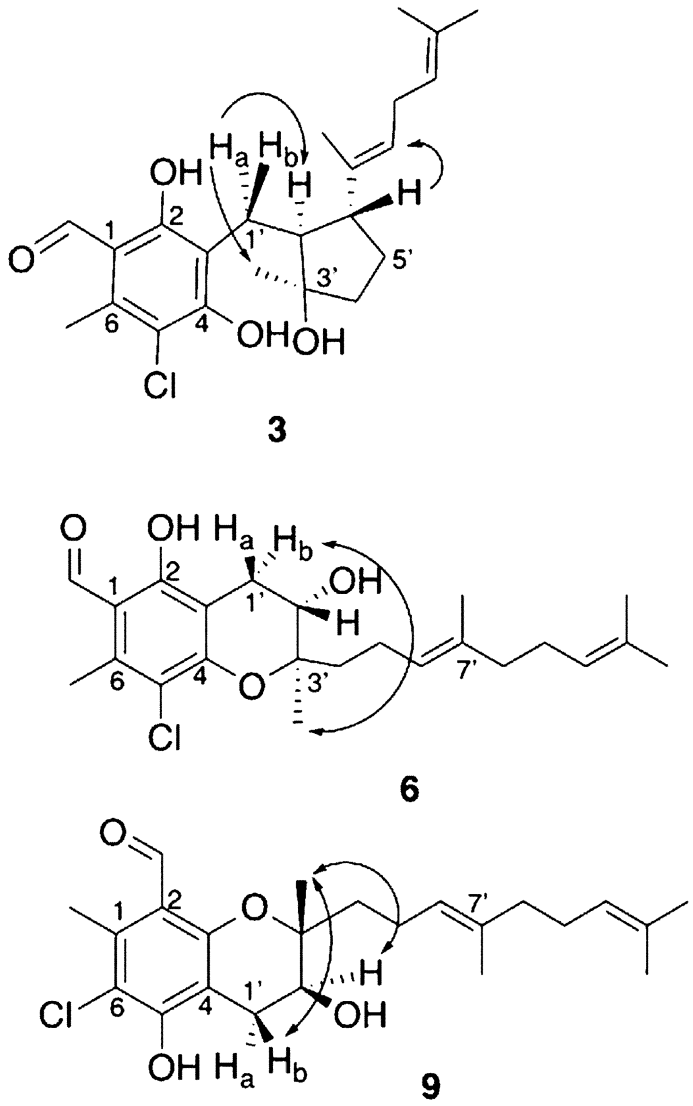

Fig. 3. Key ^{1}H-^{1}H nOe correlations of compounds **3**, **7** and **9**.

Compound **10** was obtained as a dark brown powder. Its molecular formula ($C_{23}H_{34}O_5$) was determined by HRESIMS ($[M+H]^+$ peak at *m/z* 391.2479, calcd 391.2484) suggesting seven degrees of unsaturation. The ^{1}H and ^{13}C NMR spectra revealed that compound **10** had a chromane core, same as compounds **7**, **8** and **9** (Table 2 and 3). Like compound **8**, molecule **10** had no chlorine on the aromatic and presented a proton at δ_H 6.40 ppm. Compared to compound **8**, ^{13}C NMR data revealed the presence of one additional carbinol at δ_C 69.2 ppm, and the lack of one olefinic carbon. The HMBC correlations of H12'/H13' with the carbinol mentioned above suggested that compound **10** resulted from the hydration of a C-10′−C-11′ double bond according to the Markovnikov's rule (Fig. 2). The chemical shift of the hydroxyl proton at δ_H 8.19 ppm permitted to determinate that compound **10** was cyclized on C-2.

The relative configurations of compounds **7** to **10** were determined by NMR analyses of the nOe correlations between 3′-CH_3 with H-1′b and H-2′ (Fig. 3.). Indeed, on the NOESY spectrum nOe correlations are observed between 3'-CH_3 and only one of the methylene protons H-1', and this

methylene proton does not correlate with the H-2' proton. These compounds with the chromane core were named ilicicolinal F, G, H and I.

Table 3
^{1}H NMR Spectroscopic Data for Compounds **7**−**14** (δ_H, *J* in Hz are given in parentheses).

Position	7[a]	8[a]	9[b]	10[c]	11[b]	12 [c]	13 [c]	14 [c]
1								6.46 s
5		6.23 s		6.40 s			6.05 s	
1′	2.97 dd (17.0, 5.0)	2.95 dd (14.2, 3.6)	2.96 dd (17.0, 4.7)	2.93 m	3.37 d (7.8)	3.41 d (7.2)	3.31 m	3.41 d (6.3)
	2.72 dd (17.0, 6.0)	2.69 dd (14.3, 11.4)	2.60 dd (17.0, 6.7)	2.53 m				
2′	3.94 t (5.6)	3.93 m	3.87 t (6.1)	3 .89 t (6.0)	5.28 t (6.6)	5.33 t (6.3)	5.34 t (6.3)	5.34 t (6.3)
4′	1.69 t (8.3)	1.69 m	1.71 t (7.8)	1.79 t (8.0)	1.97 d (6.3)	1.94 m	1.91 t (6.3)	1.93 t (7.2)
5′	2.21 m	2.16 m	2.19 m	2.24 dd (15.0, 7.5)	1.38 m	1.43 m	1.40 m	1.45 m
6′	5.13 t (6.8)	2.49 m	5.14 t (6.9)	5.21 t (6.5)	1.38 m	1.36 m	1.39 m	1.39 m
8′	1.97 t (7.0)	1.99 t (7.0)	1.96 t (6.9)	1.97 t (7.3)	1.38 m	1.35	1.39	1 .41
9′	2.05 m	2.73 t (6.6)	2.04 t (6.9)	5.21 t (6.5)	1.38 m	1.35 m	1.40 m	1.45 m
10′	5.08 t (6.7)	5.12 t (7.0)	5.04 t (7.1)	1.39 m	1.40 m	1.39 m	1.41 m	1.41 m
12′	1.68 s	1.65 s	1.64 br, s	1.13 s	1.16 s	1.16 s	1.14 s	1.14 s
13′	1.59 s	1.70 s	1.57 s	1.13 s	1.16 s	1.16 s	1.14 s	1.14 s
1-CHO	10.14 s	10.14 s	10.49 s	10.47 s				
1-CO_2H					nd	nd	nd	
2-OH	12.73 s	12.77 s	nd	nd	nd	nd	nd	nd
4-OH	nd	nd	8.59 br s	8.19 br s	8.12 br s	8.55 br s	8.57 br s	8.04 br s
6-CH_3	2.60 s	2.62, s	2.60, s	2.44 s	2.64 s	2.75 s	2.53 s	2.22 s
3′−CH_3	1.41 s	1.03, s	1.30, s	1.28 s	1.79 s	1.80 s	1.77 s	1.78 s
7′−CH_3	1.61 s	1.64, s	1.58, s	1.62 s	1.06 s	1.11 s	1.09 s	1.09 s

[a] Recorded at 600 MHz in $CDCl_3$.
[b] Recorded at 600 MHz in MeOD.
[c] Recorded at 600 MHz in C_5D_5N.

Compounds **11** and **12** were obtained as a light beige powder. A molecular formula of $C_{23}H_{35}ClO_6$ was determined via HRESIMS, which showed a pseudomolecular ion at *m/z* 441.2053 and 441.2047 $[M-H]^-$ (calcd 441.2044). Compound **13** had a molecular formula of $C_{23}H_{36}O_6$ and was determined via HRESIMS analysis, which showed a pseudomolecular ion at *m/z* 407.2441 $[M-H]^-$ (calcd 407.2434) and the compound **14** molecular formula of $C_{22}H_{35}O_4Cl$ was deduced from HRESIMS analysis, which showed a pseudomolecular ion at *m/z* 397.2146 $[M-H]^-$ (calcd at *m/z* 397.2146). Compounds **11-14** shared the same di-hydroxylated farnesyl side chain. Structural differences occurred on the resorcinol part with variations in the nature and position of the substituents. The structure of the side chain was deduced from the analysis of COSY correlations and the clear and intense HMBC correlations observed for the methyl groups. The methyl group of these compounds linked to 7' had δ_H around 1.06-1.11 ppm instead of 1.58 ppm for compounds **2**, and the C-7' quaternary carbon exhibited a signal around δ_c 70.9-72.0 ppm, which indicated that it carried out an oxygen. Farnesyl chain of **11-14** was hydrated across C-6—C-7'. Therefore, the COSY correlations between the methyl group at δ_H 1.14-1.16 ppm (H-12' and H13') and a carbon at δ_c 69.2-70.1 ppm (C-11') placed a tertiary alcohol in C-11'. The position and the nature of the substituents on the aromatic moiety were determined with the ^{13}C NMR data and HMBC correlations observed with 6-CH_3 as described in the literature for ilicicolinic acids A-D (Kuroda et al., 1993; Nirma et al. 2015a). And, for compound **13** and **14**, with the HMBC correlations of the aromatic proton observed at δ_H 6.05 and 6.46 respectively (Fig. 2). Compounds **11-13** were named ilicicolinic acid E, F and G, and compound **14** was named ilicinolinol.

From the 17 metabolites produced by *Neonectria discophora* SNB-CN63, the possible biosynthetic correlations among them are summarized in Fig.4. In the literature, it was reported that ilicicolin A (**2**) was biosynthesized through the mevalonate and polyketide pathways (Hunter 1978; Kawaguchi et al., 2013). In this study, we proposed for groups of key intermediates between ilicicolin A (**2**). First, an oxidation of **2** can conduct ilicicolinic acid A (Fig. 4, track 1), and a hydration of its farnesyl chain can conduct ilicicolinic acids, such as compounds **11**, **12** and **13**. Epoxide formation in the alkyl chain of compound **2**, and epoxide cyclisation with the acidic phenolic hydroxyl group at C-2 or C-4 by an S_N2 opening of the epoxide ring (6 endo-trig cyclisation) results in the formation of the compounds with a chromane core, molecules **7**, **8**, **9** and **10** (Fig. 4, track 2a). From the same epoxidate **2**, a 5-exo-trig cyclization with C-2 or C-4 can produce benzofuran cores: **1** and **3** (Fig. 4, track 2a). Finally, a 5-exo-trig cyclisation by epoxide cyclisation with a double bond of the alkyl chain gives compounds **4** to **6** with a resorcinol core (Fig. 4, track 2b). This biosynthetic pathway supported the relative configuration of compounds **1** and **3** and the configurations of molecules with a resorcinol and a chromane core.

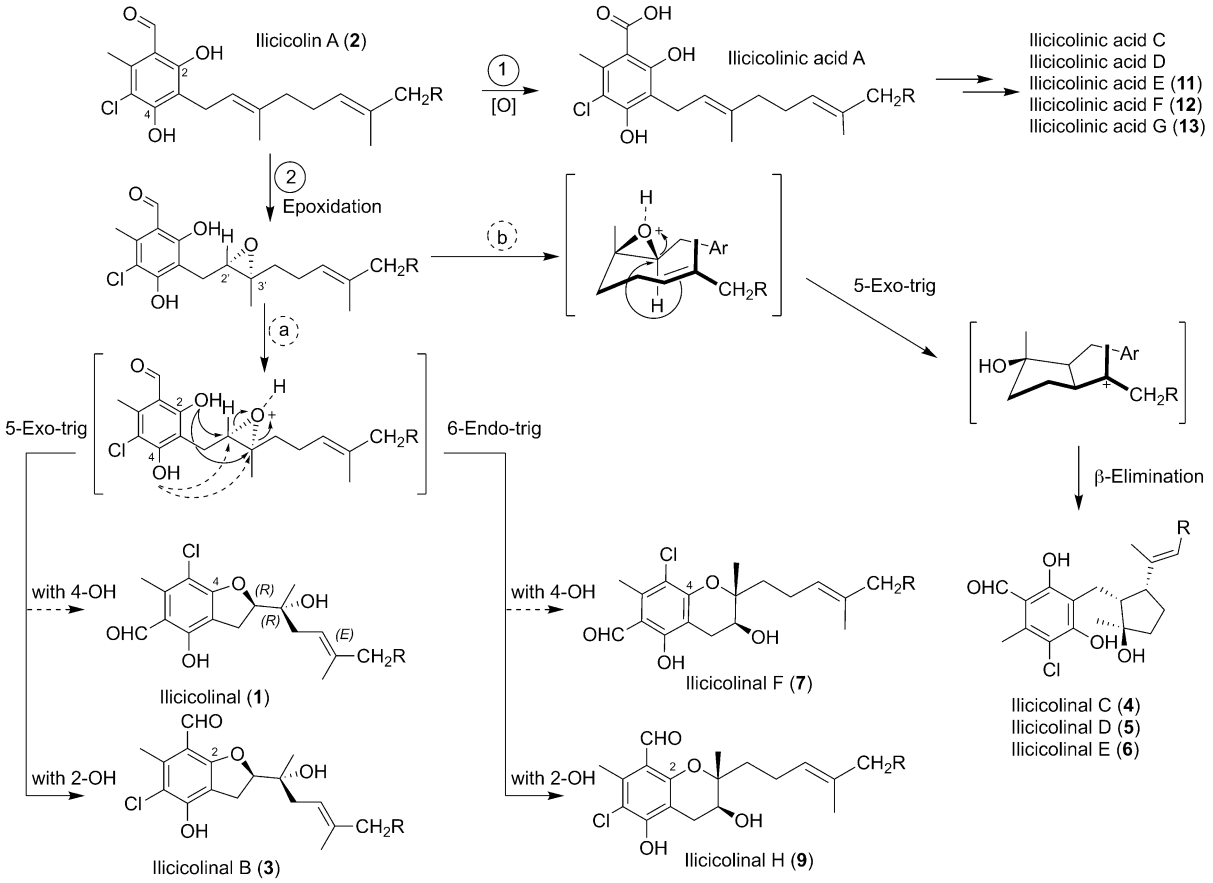

Fig. 4. Possible biosynthetic pathway to produce the compounds isolated from *Neonectria discophora* SNB-CN63.

The C-3′ configuration of **1** has never been described in the literature. To determine absolute configuration of this molecule, (*S*)- and (*R*)-MTPA esters of this compound were synthetized (respectively **1a** and **1b**), The methyl CH_3–C-3' is at δ_H 1.28 and δ_C 22.7 for the (*R*)-Mosher ester of **1**, and at δ_H 1.27 and δ_C 22.5 for the (S)-Mosher ester. Based on HMBC correlations of this methyl, it was possible to find protons H-2' (*R*: δ_H 4.776 and δ_C 91.5; *S*: δ_H 4.801 and δ_C 91.6) and H-4' (*R*: δ_H 1.43-1.51 and δ_C 37.8; *S*: δ_H 1.43-1.51 and δ_C 37.9). The analysis of protons H-2' is quite straightforward as they are well separated in the proton spectra. However, H-4' protons are a large multiplet in both case, and it was not possible to measure differences in chemical shifts even with HSQC (see supporting information). In the (*S*)-ester of compound **1**, H-2' appears more downfield than in the (*R*)-ester, and is therefore deshielded by the phenyl group. It can be concluded that C-3' is (*R*), and so is C-2' (if we assume that this compound is generated by a SN_2 on an epoxide) (Fig. 4). Finally, if we take into account the absolute configuration determined for compound **1**, and if we consider that all the compounds come from the formation of the same epoxide, we can deduce the absolute configurations of compounds **1**-**10**, as being 2'*R*, 3'*R* for **3**; 2'*S*, 3'*R* for compounds with a chromane core (**7**-**10**), and 2'*R*, 3'*R* and 6'*R* for compounds **4**, **5** and **6**.

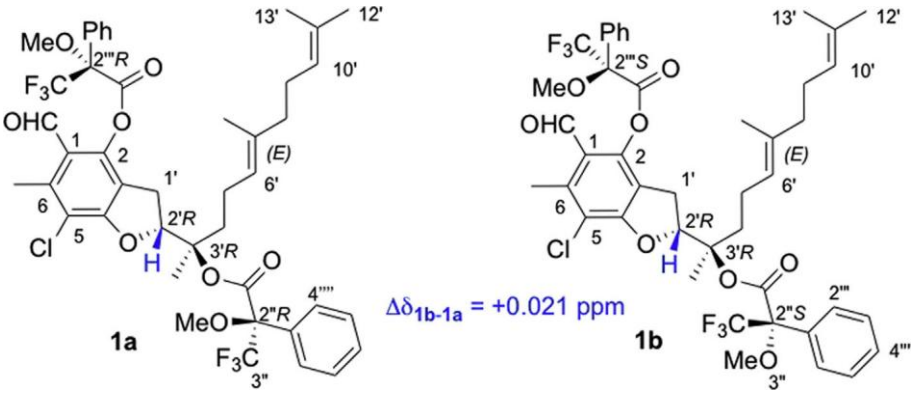

Fig. 5. *R*-MTPA (**1a**) and *S*-MTPA (**1b**) esters of **1**.

All the isolated compounds were tested on *Trichophyton rubrum* and *Staphylococcus aureus* human pathogens (Table 4). Overall, the antimicrobial activities of compounds **1** to **14** were moderate to good, depending on the strain tested. We demonstrate that compounds **3**, **4**, **5**, **10**, **11**, **12** and **14** have antimicrobial activities less than 32 µg/mL. These molecules show significant activities against *S. aureus* and/or MRSA (Methicillin-resistant *Staphylococcus aureus*), with vancomycin as a positive control, with the best MIC for **4** at 8 µg/mL. Contrary to other compounds, molecules **11** and **12** showed growth inhibition on *T. rubrum* with a MIC at 8 µg/mL too. If we compare ilicicolinic acids **11** to **14**, it seems clear that the presence of the chlorine element is necessary to have activity against *T. rubrum* (by comparison between **11** and **13**), and

carboxylic acid is necessary for activity against MRSA (by comparison between **11** and **14**). This structure-activity relationship against *S. aureus* and MRSA between compounds **1** to **14** is not clear, but we observed that the presence of a C-11′ hydroxyl group (as in molecules **10**, **11**, **12** and **14**) or the cyclisation between C-2 and C-3′ (as compounds **9** and **10**) allow us to determine that the hydroxyl in position C-4 and/or the C-11′ groups are important for these antimicrobial activities. Finally, if we compare compounds **3** to **5**, it seems that the proton configuration of H-8 is important for having activity against MRSA. We also tested the cytotoxicity on studied MRC5 and KB cell strain extracts and fractions, on which we detected inhibition growth <20% at 1 µg/mL (See supporting information).

3. Conclusion

In conclusion, this article provides the first description and isolation of 4 new ilicicolonic acids (**11**-**14**) and 8 original ilicicolinal derivatives (compounds **3**-**10**). Contrary to compound **1**, ilicicolin A (**2**) was isolated from other natural products: *Cylindrocarpon* sp. and *Fusarium* sp. (filamentous fungi), which were isolated from soil samples (Ellestad et al., 1969; Mori and Fujioka, 1984; Kawaguchi et al., 2013). Prenylated phenols are known for their antibiotic properties, and compound **2** was previously synthetized. Compound **2** is also described in the literature as anti-protozoan, antineoplastic and as a dihydroorotic acid dehydrogenase inhibitor (Saimoto et al., 2013, 2015). In our study, we detail for the first time complete NMR ^{1}H and ^{13}C and 2D data on this molecule. From ilicicolin A, we have been able to propose a biosynthetic pathway for all the new isolated molecules from *Neonectria discophora* extract. This biosynthetic pathway allowed us to deduce the configuration of all the isolated compounds. Moreover, the absolute configuration of the compound **1** was determined for the first time. Finally, six compounds had antibacterial activities against MRSA, and two compounds had antifungal activity against *T. rubrum* with MIC < 16 µg/mL: ilicicolinal C, D, E and I and ilicicolinic acid E and F.

This finding may inspire the discovery of new and selective antibacterial agents. These compounds were obtained from a *Neonectria discophora* strain isolated from an aerial nest of *Nasutitermes corniger*. It is reasonable to hypothesize that this microbe provided its host with effective antimicrobial protection. The biosynthetic pathway it utilized by this microbe and whether this strain is shared by other colonies is a question that remains to be addressed.

4. Experimental

4.1. General experimental procedures

Optical rotations were measured on an Anton Paar MCP 300 polarimeter in a 100 mm-long 350 µL cell. Nuclear Magnetic Resonance (NMR) spectra were recorded on a Bruker 500 MHz spectrometer or a Bruker 600 MHz spectrometer equipped with a 1-mm inverse detection probe.

Chemical shifts (δ) are reported as ppm based on the TMS signal, and the coupling constants (*J*) are reported in Hertz. HR-ESI-MS measurements were performed using a Waters Acquity UPLC system with a column bypass coupled to a Waters Micromass LCT Premier Time-of-Flight mass spectrometer (Milford, MA, USA) equipped with an electrospray interface (ESI). Flash chromatography was performed on a Grace Reveleris system with dual UV and ELSD detection equipped with an 80 g silica column. For UV-based experiments, effluents were monitored at 254 and 280 nm. Analytical and preparative HPLCs were conducted with a Gilson system equipped with a 322 pumping device, a GX-271 fraction collector, a 171 diode array detector and a prepELSII detector electrospray nebulizer. Columns used for these experiments included a Phenomenex Luna C_{18} 5 µm 4.6 x 250 mm, Phenomenex PFP 5 µm 4.6 x 250 mm analytical column, Phenomenex Luna C_{18} 5 µm 21.2 x 250 mm and PFP 5 µm 21.5 x 250 mm preparative column. The flow rate was set to 1 or 17 mL/min using a linear gradient of water mixed with an increasing proportion of acetonitrile. All solvents were HPLC grade. UV spectra were recorded using a Perkin-Elmer Lamba 5 spectrophotometer. The CD spectra were measured at 25°C on a JASCO J-810 spectropolarimeter. Potato Dextrose Agar (PDA) was purchased from Fluka Analytical.

4.2. Collection and identification of Neonectria discophora *SNB-CN63.*

N. discophora was collected, identified and preserved as described in the literature (Nirma et al., 2015a). The strain was isolated from an *N. corniger* termite aerial nest, sampled in Rémire-Montjoly, French Guiana, in 2011. A piece of the nest matter was placed in supsension in sterile water, and this solution was spread on PDA medium placed in Petri dishes. After 7 days of incubation at 25°C, the first fungus hyphae were removed and transferred to another Petri dishes. The colony is maintained in triplicate at -80°C in glycerol-Water (50/50). A sample was submitted for amplification and nuclear ribosomal internal transcribed spacer ITS4 sequencing allowed for strain identification by NCBI sequence comparison. The ITS4 sequence has been registered in the NCBI GenBank database (http://www.ncbi.nlm.nih.gov) under registry number KJ023733. Molecular analyses were performed externally by BACTUP, France.

4.3. Culture, extraction and isolation

The *N. discophora* strain was cultivated on PDA at 26°C for 15 days, initially on a small scale and then on 150 Petri dishes (of 14-cm diameter). The fungus and culture medium were then transferred into a large container and macerated with ethyl acetate for 24 h. The organic solvent was then collected by filtration, washed with water in a separating funnel and evaporated, yielding 0.92 g of crude extract. A portion of the crude extract (803 mg) was purified by flash chromatography with a linear gradient of hexane-AcOEt followed by another gradient of AcOEt-MeOH. Six fractions were gathered based on their TLC profiles. Fractionation of fraction IV on

the C_{18} prep-HPLC with ACN/Water gradient (87/13 to 100/0) in 15 min permitted to obtain compound **1** (91.5 mg, rt 14.1 min), **2** (8.6 mg, rt 17.3 min) and **7** (8.1 mg, rt 16.6 min). Two sub-fractions were submitted to PFP HPLC-prep in other conditions (ACN/Water 75/25 to 100 % in 24 min) to give compounds **9** (1.8 mg, rt 6.6 min) and **4** (1.2 mg, rt 11.0 min) from the first fraction and compound **6** (0.8 mg, rt 8.2 min) from the second. Purification of fraction II with C_{18} prep-HPLC with isocratic ACN/water for 4 min followed by a gradient of 87/13 to 100/0 for 15 min permitted to isolate **14** (3.1 mg, rt 8.7), **10** (0.9 mg, rt 9.6 min), **13** (1.5 mg, rt 12.5), **11** (2.6 mg, rt 12.9) and **12** (3.3 mg, rt 15.2). Fractionation of fraction VI on a C_{18} prep-HPLC with an ACN/Water gradient (80/20 to 83/17) in 30 min gave compounds **5** (0.5 mg, rt 10.4 min), **3** (0.9 mg, rt 11.0 min), and **8** (0.7 mg, rt 15.2).

*4.4. Ilicicolinal (**1**)*

Dark red oil; $[\alpha]^{25}_{D}$ +99 ($CHCl_3$; c 0.1); UV (λ_{max} $CHCl_3$) (log ε) 240 nm (3.2), 302 (3.6); ^{1}H NMR: 3.22 m (H-1′), 4.87 dd (8.5, 9.8) (H-2′), 1.55 t (8.4) (H-4′), 2.14 m (H-5′a), 2.18 m (H-5′b), 5.14 t (6.8) (H-6′), 1.98 m (H-8′), 2.09 t (6.3) (H-9′a), 1.97 m (H-9′b), 5.08 t (6.8) (H-10′), 1.77 s (H-12′), 1.60 s (H-13′), 10.14 s (1-CHO), 12.48 s (2-OH), 2.59 s (6-CH_3), 1.35 s (3′-CH_3), 1.63 s (7′-CH_3), 1.35 (3′-CH_3) see supporting information; ^{13}C NMR: 114.6 (C-1), 159.4 (C-2), 112.2 (C-3), 163.4 (C-4), 108.3 (C-5), 141.3 (C-6), 27.4 (C-1′), 91.7 (C-2′), 73.6 (C-3′), 36.9 (C-4′), 21.8 (C-5′), 123.7 (C-6′), 136.0 (C-7′), 39.6 (C-8′), 26.6 (C-9′), 124.1 (C-10′), 131.5 (C-11′), 25.7 (C-12′), 17.7 (C-13′), 14.0 (6-CH_3), 22.7 (3′-CH_3), 16.0 (7′-CH_3); HRESIMS $[M+H]^+$ *m/z* 407.1992 (calcd for $C_{23}H_{32}ClO_4$ *m/z* 407.1989).

*4.5. Ilicicolin A (**2**)*

White pink powder; $[\alpha]^{25}_{D}$ 0 (c 0.1, MeOH); UV (λ_{max} $CHCl_3$) (log ε) 210 nm (3.0) 240 nm (3.3), 293 nm (3.5); NMR spectral data, see supporting information and Tables 1 and 2; HRESIMS $[M+H]^+$ *m/z* 391.2034 (calcd for $C_{23}H_{32}ClO_3$ *m/z* 391.2040).

*4.6. Ilicicolinal B (**3**)*

Dark purple oil; $[\alpha]^{25}_{D}$ +21 (c 0.1, $CHCl_3$); UV (λ_{max} $CHCL_3$) (log ε) 240 nm (1.7), 301 nm (2.6); NMR spectral data, see supporting information and Tables 1 and 2; HRESIMS $[M+H]^+$ *m/z* 407.1991 (calcd for $C_{23}H_{32}ClO_4$ *m/z* 407.1989).

*4.7. Ilicicolinal C (**4**)*

Yellow oil; $[\alpha]^{25}_{D}$ +67 (c 0.1, MeOH); UV (λ_{max} $CHCl_3$) (log ε) 240 nm (3.1), 300 nm (3.4); NMR spectral data, see supporting information and Tables 1 and 2; HRESIMS $[M-H]^-$ *m/z* 405.1821 (calcd for $C_{23}H_{30}ClO_4$ 405.1834).

*4.8. Ilicicolinal D (**5**)*

Dark purple powder; $[\alpha]^{25}_{D}$ +68 (c 0.05, $CHCl_3$); UV (λ_{max} $CHCl_3$) (log ε) 239 nm (3.1), 287 nm (3.7); NMR spectral data, see supporting information and Tables 1 and 2; HRESIMS $[M-H]^-$ *m/z* 405.1828 (calcd for $C_{23}H_{30}ClO_4$ *m/z* 405.1833).

*4.9. Ilicicolinal E (**6**)*

Dark purple powder; $[\alpha]^{25}_{D}$ +70 (c 0.1, $CHCl_3$); UV (λ_{max} $CHCl_3$) (log ε) 239 nm (2.7), 297 nm (3.0), 344 nm (2.2); NMR spectral data, see supporting information and Tables 1 and 2; HRESIMS $[M-H]^-$ *m/z* 405.1842 (calcd for $C_{23}H_{30}ClO_4$ *m/z* 405.1833).

*4.10. Ilicicolinal F (**7**)*

Brown oil; $[\alpha]^{25}_{D}$ −24 (c 0.1, MeOH); UV (λ_{max} $CHCl_3$) (log ε) 213 nm (3.4); NMR spectral data, see supporting information and Tables 2 and 3; HRESIMS $[M+H]^+$ *m/z* 407.1993 (calcd for $C_{23}H_{32}ClO_4$ *m/z* 407.1989).

*4.11. Ilicicolinal G (**8**)*

Yellow oil; $[\alpha]^{25}_{D}$ −100 (c 0.1, MeOH); UV (λ_{max} $CHCl_3$) (log ε) 240 nm (3.1), 299 nm (3.6); NMR spectral data, see supporting information and Tables 2 and 3; HRESIMS $[M+H]^+$ *m/z* 373.2374 (calcd for $C_{23}H_{33}O_4$ *m/z* 373.2379).

*4.12. Ilicicolinal H (**9**)*

Dark purple powder; $[\alpha]^{25}_{D}$ −6 (c 0.05, $CHCl_3$); UV (λ_{max} $CHCl_3$) (log ε) 239 nm (3.5), 278 nm (2.8), 324 nm (1.1); NMR spectral data, see supporting information and Tables 2 and 3; HRESIMS $[M+H]^+$ *m/z* 407.1994 (calcd for $C_{23}H_{32}ClO_4$ *m/z* 407.1989).

4.13. *Ilicicolinal I (**10**)*

Brownish powder; $[\alpha]^{25}_{D}$ +30 (c 0.1, MeOH); UV (λ_{max} $CHCl_3$) (log ε) 223 nm (3.5), 286 (3.3); NMR spectral data, see supporting information and Tables 2 and 3; HRESIMS $[M+H]^+$ *m/z* 391.2479 (calcd for $C_{23}H_{35}O_5$ *m/z* 391.2484).

*4.14. Ilicicolinic acid E (**11**)*

Beige powder; $[\alpha]^{25}_{D}$ −3 (c 0.06, MeOH); UV (λ_{max} MeOH) (log ε) 220 nm (3.9), 306 nm (3.1); NMR spectral data, see supporting information and Tables 2 and 3; HRESIMS $[M-H]^-$ *m/z* 441.2053 (calcd for $C_{23}H_{34}ClO_6$ *m/z* 441.2044).

*4.15. Ilicicolinic acid F (**12**)*

Beige powder; $[\alpha]^{25}_{D}$ −112 (c 0.01, MeOH); UV (λ_{max} MeOH) (log ε) 222 nm (3.8), 304 nm (3.2); NMR spectral data, see supporting information and Tables 2 and 3; HRESIMS $[M-H]^-$ *m/z* 441.2047 (calcd for $C_{23}H_{34}ClO_6$ *m/z* 441.2044).

*4.16. Ilicicolinic acid G (**13**)*

Beige powder; $[\alpha]^{25}_{D}$ −80 (c 0.02, MeOH); UV (λ_{max} MeOH) (log ε) 222 nm (3.8), 299 (3.2); NMR spectral data, see supporting information and Tables 2 and 3; HRESIMS $[M-H]^-$ *m/z* 407.2441 (calcd for $C_{23}H_{35}O_6$ *m/z* 407.2434).

*4.17. Ilicicolinol (**14**)*

Beige powder; $[\alpha]^{25}_{D}$ −8 (c 0.03, MeOH); UV (λ_{max} MeOH) (log ε) 205 nm (3.1); NMR spectral data, see supporting information and Tables 2 and 3; HRESIMS $[M-H]^-$ *m/z* 397.2146 (calcd for $C_{22}H_{34}ClO_4$ *m/z* 397.2146).

For compounds **3**, **6** and **8**-**10** ^{13}C chemical shifts were deduced from proton-carbon correlation experiments.

*4.18. MTPA derivatives of **1***

In an NMR sample tube (3 mm diameter) 1 mg of dimethylamynopyridine (DMAP) was added to 1.0 mg of compound **1**. Nine microliter of pyridine-d_5 and 600 µl of $CDCl_3$ were added to this mixture. Then, 1.35 µl of (*R*)-MTPA chloride was added. The resultant reaction mixture was allowed to stand at RT for 120 min, to afford (*S*)-MTPA ester **1a**. The reaction was monitored directly by NMR and upon completion, the chemical shifts of the relevant protons were obtained directly from ^1H and 2D NMR experiments. The identical procedure was carried out to obtain the (*R*)-MTPA **1b** ester from (*S*)-MTPA chloride.

4.19. Antimicrobial assays.

The ATCC strains were purchased, and the clinical isolate was provided by Prof. P. Loiseau, at the University Paris Sud (ITS sequence deposited in the NCBI GenBank database under the registry number KC692746 corresponding to SNB-TR1 strain). Crude extracts, fractions and pure compounds were tested according to the reference protocol of the European Committee on Antimicrobial Susceptibility Testing (EUCAST, 2003, 2008). The MIC value was obtained after 18 h for yeasts, 5 days for *T. rubrum* and 24 h for *S. aureus*.

4.20. Cytotoxicity assays.

The cytotoxicity assays were conducted with the KB (nasopharyngeal epidermoid carcinoma) and MRC5 (Human Fetal Lung Fibroblast) cell lines according to the procedure described by Tempête et al. with the positive control Taxotère (with IC_{50} = 0.2 and 0.5 nM respectively) (Tempête et al., 1995).

5. Acknowledgment

This work has benefited from an "Investissement d'Avenir" grant managed by Agence Nationale de la Recherche [CEBA, ref. ANR-10-LABX-0025].

Appendix A. Supplementary data

Experimental methods, full spectroscopic data and NMR spectra of compounds **1**-**14** can be found at http://dx.doi.org/.

References

Adnani, N., Rajski, S.R., Bugni, T.S., 2017. Symbiosis-inspired approaches to antibiotic discovery. Nat. Prod. Rep. 34, 784–814.

Beemelmanns, C., Guo, H., Rischer, M., Poulsen, M., 2016. Natural products from microbes associated with insects. Beilstein J. Org. Chem. 12, 314–327.

Berenbaum, M.R., Eisner, T., 2008. Ecology. Bugs' bugs. Science 322, 52–53.

Borysowski, J., Górski, A., 2008. Is phage therapy acceptable in the immunocompromised host? Int J Infect Dis. 12, 466–471.

Currie, C.R., Poulsen, M., Mendenhall, J., Boomsma, J.J., Billen, J., 2006. Coevolved crypts and exocrine glands support mutualistic bacteria in fungus-growing ants. Science 311, 81–83.

Davies, G.R., Hope, W., Khoo, S., 2013. Opinion: the pharmacometrics of infectious disease. CPT Pharmacometrics Syst Pharmacol. 2:e70. doi:10.1038/psp.2013.46.

Ellestad, G.A., Evans Jr., R.H., Kunstmann, M.P., 1969. Some new terpenoid metabolites from an unidentified *Fusarium* species. Tetrahedron 25, 1323–1334.

European Committee for Antimicrobial Susceptibility Testing (EUCAST) of the European Society for Clinical Microbiology and Infectious Diseases (ESCMID). EUCAST Discussion Document E. Dis 5.1: determination of minimum inhibitory concentrations (MICs) of an, 2003. Determination of minimum inhibitory concentrations (MICs) of antibacterial agents by broth dilution, Clin Microbiol Infec. 9, 1-7.

European Committee for Antimicrobial Susceptibility Testing (EUCAST), Subcommittee on Antifungal Susceptibility Testing (AFST) of the ESCMID European Committee for Antimicrobial Susceptibility Testing (EUCAST) 2008. EUCAST definitive document EDef 7.1: method for the determination of broth dilution MICs of antifungal agents for fermentative yeasts. Clin Microbiol Infect. 14, 398–405.

Gutiérrez, M., Theoduloz, C., Rodríguez, J., Lolas, M., Schmeda-Hirschmann, G., 2005. Bioactive Metabolites from the Fungus *Nectria galligena*, the Main Apple Canker Agent in Chile. J. Agric. Food Chem. 53, 7701–7708.

Hashimoto, T., Quan, D.N., Nukada, M., Nukada, M., Asakawa, Y., 2005. Isolation, synthesis and biological activity of grifolic acid derivatives from the inedible mushroom *Albatrellus dispansus*. Heterocycles 65, 2431–2439.

Hunter, R., Mellows, G., 1978. Detection of deuteride shifts in the biosynthesis of the fungal triprenylphenol, ascochlorin, by 13C nuclear magnetic resonance spectroscopy following incorporation of [3-13C, 4-2H2] - mevalonic acid. Tetrahedron Lett. 19, 5051–5054.

Kawaguchi, M., Fukuda, T., Uchida, R., Nonaka, K., Masuma, R., Tomoda, H., 2013. A new ascochlorin derivative from *Cylindrocarpon* sp. FKI-4602. J. Antibiot. (Tokyo). 66, 23–29.

Martinez-Rossi, N.M., Peres, N.T., Rossi, A., 2008. Antifungal resistance mechanisms in dermatophytes. Mycopathologia 166, 369–383.

Matsui, T., Tanaka, J., Namihira, T., Shinzato, N., 2012. Antibiotics production by an actinomycete isolated from the termite gut. J Basic Microbiol. 52, 731–735.

Mori, K., Takafumi, F., 1984. Synthesis of (±)-ascochlorin, (±)-ascofuranone and LL-Z1272. Tetrahedron 40, 2711–2720.

Nirma, C., Eparvier, V., Stien, D., 2013. Antifungal agents from *Pseudallescheria boydii* SNB-CN73 isolated from a *Nasutitermes* sp. termite. J. Nat. Prod. 76, 988–991.

Nirma, C., Eparvier, V., Stien, D., 2015. Antibacterial ilicicolinic acids C and D and ilicicolinal from *Neonectria discophora* SNB-CN63 isolated from a termite nest. J. Nat. Prod. 78, 159–162.

Nirma, C., Eparvier, V., Stien, D., 2015. Reactivation of antibiosis in the entomogenous fungus *Chrysoporthe* sp. SNB-CN74. J. Antibiot. (Tokyo). 68, 586–590.

Purvis, A., Hector, A., 2000. Getting the measure of biodiversity. Nature 405, 212–219.

Ramadhar, T.R., Beemelmanns, C., Currie, C.R., Clardy, J., 2014. Bacterial symbionts in agricultural systems provide a strategic source for antibiotic discovery. J. Antibiot. (Tokyo). 67, 53–58.

Saimoto, H., Kita, K., Yabu, Y., Yamamoto, M., 2015. Dihydroorotic acid dehydrogenase inhibitor. EP2857010.

Saimoto, H., Kita, K., Yabu, Y., Yamamoto, M., 2013. Novel dihydroxybenzene derivatives and antiprotozoal agent comprising same as active ingredient. EP 2636663 A1.

Stow, A., Briscoe, D., Gillings, M., Holley, M., Smith, S., Leys, R., Silberbauer, T., Turnbull, C., Beattie, A., 2007. Antimicrobial defences increase with sociality in bees. Biol Lett. 3, 422–424.

Stow, A., Beattie, A., 2008. Chemical and genetic defenses against disease in insect societies. Brain Behav Immun. 22, 1009–1013.

Takamatsu, S., Rho, M.C., Masuma, R., Hayashi, M., Komiyama, K., Tanaka, H., Omura, S., n.d. A novel testosterone 5α-reductase inhibitor, 8′,9′-dehydroascochlorin produced by *Verticillium* sp. FO-2787. Chem Pharm Bull. 42, 953–956.

Tempête, C., Werner, G.H., Favre, F., Rojas, A., Langlois, N., 1995. In vitro cytostatic activity of 9-demethoxyporothramycin B. Eur. J. Med. Chem. 30, 647–650.

Zhang, P., Bao, B., Dang, H.T., Hong, J., Lee, H.J., Yoo, E.S., Bae, K.S., Jung, J.H., 2009. Anti-inflammatory sesquiterpenoids from a sponge-derived fungus *Acremonium* sp. J. Nat. Prod. 72, 270–275.